# Dose-Wise Scanning in Visceral Computed Tomography Angiography

## A Phantom Study

Thomas Werncke, MD,\* Christian von Falck, MD,† Matthias Taupitz, MD,\* Christoph Hoeschen, PhD,‡ Frank Wacker, MD,† and Bernhard Christian Meyer, MD†

Objectives: The aim of this study was to analyze the influence of the tube current-time product in multidetector computed tomography angiography on the accuracy of stenosis quantification in a phantom model of occlusive vessel disease

Materials and Methods: Stenosed pelvic and visceral arteries were simulated using acrylic tubes (inner diameter: small, 4.0 mm; large, 6.5 mm) filled with plaque material (epoxy resin, hydroxylapatite, glass bubbles) to create different degrees of stenosis and plaque composition (calcified plaques, >1000 Hounsfield units [HU]; soft plaques, ~50 HU; inhomogeneous plaques, 50–1000 HU). The lumen was filled with water-diluted contrast material (Iomeprol 400; Bracco Imaging, Konstanz, Germany) to increase the density to 350 HU. The vessel phantoms were inserted in an Alderson phantom and imaging was conducted on a 64-slice MDCT (Somatom Definition, Siemens, Forchheim, Germany; collimation, 0.6 mm; reconstructed slice thickness, 1 mm; 120 kVp) using 8 different image acquisition protocols (IAPs), with reference tube current-time products (I<sub>QualRef</sub>) ranging between 20 and 280 mAs (IAP<sub>20</sub>-IAP<sub>280</sub>). The signal-to-noise ratio was calculated for each IAP. The measured luminal area within a stenosis was correlated to the known value using the Kappa-Lin test ( $\kappa_{Lin}$ ). A decrease of 10% of the maximum achievable correlation was defined as substantial. The sensitivity and specificity of hemodynamically relevant stenoses (>50%) were computed. For all IAPs, the effective dose was measured with thermoluminescence dosimetry and calculated with CTEXPO 2.0 (ICRP103).

Results: The measured effective dose ranged from 0.8 to 10.7 mSv. The calculated effective dose was approximately 10% lower for each IAP (0.7-9.8 mSv). A total of 2592 stenosis measurements were performed. In large vessels, the correlation was almost perfect for IAP $_{80}$  to IAP $_{280}$  ( $\kappa_{Lin}$  = 0.91–0.95). In comparison, overall correlation was inferior in small vessels and was substantial for IAP<sub>280</sub> to IAP<sub>120</sub> ( $\kappa_{\text{Lin}} = 0.89 - 0.82$ ). Overall, the best correlation was observed in calcified ( $\kappa_{Lin} = 0.95$ ) and soft ( $\kappa_{Lin} = 0.93$ ) plaques as compared with inhomogeneous ( $\kappa_{Lin} = 0.89$ ) plaques. A substantial decrease in the correlation was observed below  $IAP_{100}$  for the large vessel phantoms and  $IAP_{120}$  for the small vessel phantoms. The sensitivity of hemodynamically relevant stenoses was 90% to 99% for IAP20 to IAP280 and both vessel diameters, whereas the specificity decreased from 91% (IAP280) to 31% (IAP20) for the large vessel phantoms and from 81% to 25%, respectively, for the smaller vessel phantoms.

Conclusion: In large (>6.5 mm) vessel phantoms that simulate pelvic and renal arteries, representing a high-contrast scenario, a substantial dose reduction is

Received December 14, 2011; and accepted for publication, after revision, April 14,

Conflicts of interest and source of funding: This study was funded by the German Federal Ministry for Education and Research (Bundesministerium für Bildung und Forschung) through grant 02NUK008D (www.helmholtz-muenchen.de/kvsf/). The authors report no conflicts of interest.

Reprints: Thomas Werncke, MD, Klinik und Hochschulambulanz für

Radiologie, Charité Universitaetsmedizin Berlin, Campus Benjamin Franklin, Hindenburgdamm 30, 12200 Berlin, Germany. E-mail: Thomas.Werncke@

Copyright © 2012 by Lippincott Williams & Wilkins

ISSN: 0020-9996/12/4709-0530

feasible as compared with established abdominal imaging protocols. In smaller vessel phantoms that represent intestinal arteries, the quality of luminal delineation is already limited because of the spatial resolution. Therefore, an increase in image noise can only be accepted to a smaller degree and the potential dose reduction is limited but still substantial.

Key Words: CT angiography, phantom study, low-dose, abdominal, TLD, dosimetry

(Invest Radiol 2012;47: 530-537)

M ultislice computed tomography angiography (CTA) and magnetic resonance angiography (MRA) are highly accurate for the evaluation of abdominal vessels. 1-4 The invasive digital substraction angiography as the gold standard is therefore being increasingly replaced by the noninvasive CTA and MRA.5 Duplex ultrasound as another imaging modality has a lower accuracy as compared with MRA and CTA and is subject to higher interobserver variation and longer examination times.6

Shorter examination times, less frequent interruption of image acquisition caused by claustrophobia, continuous availability in the emergency setting, and lower costs of CTA compared with MRA have led to a wide acceptance of CTA.<sup>7</sup>

A major disadvantage of CTA is the need for ionizing radiation. In recent years, different techniques, such as automatic exposure control, adaptive dose shields reducing the overranging and overbeaming effect, and new iterative reconstruction algorithms, have been introduced to keep dose in computed tomography (CT) "as low as reasonable achievable" (ALARA principle).8-13

A key principle in terms of dose-wise CT scanning is to adjust the dose application and, thus, the image quality to the specific diagnostic task. 14 Several studies have proven the diagnostic value of low-dose CT protocols based on low tube current (low-mAs) or low tube voltage (low-kVp) compared with the standard parameters if highcontrast objects are subject of interest.

In several settings, such a high contrast is intrinsic, for example, in virtual CT colonoscopy, chest CT for pulmonary nodule detection, or abdominal CT for urinary tract calculi detection. In these situations, a dose reduction between 70% and 90% compared with the standard protocols for lung nodule detection and for virtual CT colonoscopy is feasible without a significant reduction in sensitivity and specificity. 15-17 In CTA, a high-contrast situation is usually achieved by an optimized contrast agent administration that leads to a strong luminal enhancement. Watanabe et al<sup>18</sup> showed that increasing the enhancement by using higher iodine delivery rates allows for a reduction of the radiation exposure by approximately 30% in abdominal CT. Especially in biphasic abdomen protocols, where soft tissue information is derived mainly from the portal-venous phase, a lower signal-to-noise ratio (SNR) may be tolerated for the arterial phase if the depiction of the vessel architecture is the primary task. Comparable with lung nodules in the surrounding aerated lung parenchyma or bowel wall polyps in CT colonoscopy, contrast-enhanced vessels show a high luminal contrast to the surrounding tissue. When compared with standard abdominal CT, CTA acquisition protocols therefore bear

From the \*Klinik und Hochschulambulanz für Radiologie, Charité Universitaetsmedizin Berlin, Berlin; †Department of Radiology, Medical School Hannover, Hannover; and ‡Department of Medical Radiation Physics and Diagnostics, Helmholtz Zentrum München, German Research Center for Environmental Health, Neuherberg, Germany.

a high potential of dose reduction, in particular if large vessels, such as the aorta or the iliac arteries, are of interest. Because of this fact, the default CTA IAPs of many CT scanners already propose a reduced tube current-time product. However, various CTA protocols are used for abdominal CTA. For example, for renal arteries, the proposed protocols as reported in the literature range between a volume CT dose index (CTDI<sub>Vol</sub>) of 6.3 mGy (80 mAs) for a 4-row CT (Siemens Volume Zoom) and CTDI<sub>Vol</sub> of 25 mGy. 19,20 As of today, the effects of the applied patient dose on the accuracy of stenosis quantification have received little attention.

Despite the fact that there are several studies investigating the dependency of radiation dose and image quality of CTA for the assessment of restenosis, there is only 1 previous study in the literature facilitating a 4-row CT that analyzes the tradeoff between radiation exposure and luminal delineation of the arterial vessel in visceral and peripheral CTA.21-23

Therefore, the aim of our study was to analyze the influence of the tube current-time product on the accuracy of stenosis quantification in a phantom model of occlusive vessel disease to derive a reasonable acquisition protocol for imaging abdominal vessels.

#### **MATERIALS AND METHODS**

#### **Phantom Design**

Vessel phantoms were built as previously described<sup>24</sup> using acrylic tubes of 2 different diameters (outer diameter: small, 5.0 mm; large, 8.0 mm; inner diameter: small, 4.0 mm; large, 6.5 mm). As plaque material, a low-viscosity epoxy resin combined with an ammonium-based harder was modified with glass bubbles and calcium hydroxyl apatite to simulate soft (plaque density, 50 Hounsfield units [HU]) and calcified (plaque density, ~1000 HU) plaques. Inhomogeneous plaques were prepared by cutting calcified plaques into small pieces and embedding them in soft plaques. The acrylic tubes were filled with the plaque material. After hardening of the epoxy resin, the cylindrical plaque material was removed from the acrylic tubes, and circular, semicircular, and stairstep-like stenoses with varying degrees (mild stenosis, 0%-25%, moderate stenosis, 25%-50%; severe ste-

nosis, 50%-75%; heavy stenosis, 75%-99% and occlusion) were generated for both vessel phantom diameters by drilling holes and filling. The known luminal stenosis area by preparation was verified for each stenosis with a high-resolution CT protocol in air (tube voltage, 120 kVp; 300 mAs; collimation, 0.3 mm; no automatic tube current modulation; field of view, 150 mm; sharp kernel, U75). For each plaque composition and vessel diameter, 8 mild to moderate and 8 severe to heavy stenoses and 1 occlusion were simulated, resulting in a total of 108 equally distributed stenoses (Fig. 1). The stenoses were reinserted into 50 acrylic tubes and fixed with a thin layer of epoxy resin if necessary. Saline-diluted contrast material (Iomeprol 400; Bracco Imaging, Konstanz, Germany) was filled into the created vessel lumen to generate a luminal density of 350 HU, mimicking a representative vessel enhancement as known from abdominal CTA obtained with 120 kVp after intravenous application of Iomeprol 400 in patients with a body mass index of 25 kg/m<sup>2</sup> during the arterial phase.<sup>25</sup>

## Thermoluminescence Dosimetry

Dose and phantom measurements were performed using an anthropomorphic whole-body Alderson phantom (Alderson Research Laboratories Inc; Long Island City, NY) positioned on a vacuum mattress. The Alderson phantom consists of a human skeleton embedded in radioequivalent soft tissue material and represents a 73-kg man. For dosimetric measurements, 150 thermoluminescence detectors (TLDs) 100H (1 × 1 × 6 mm, LiF:MgCuP; TLD Poland, Krakow, Poland) were used. Thermoluminescence detectors were calibrated for absorbed dose in water using conventional x-ray equipment (SRO 2550; Philips, Medizin Systeme GmbH, Hamburg, Germany) with a tube potential of 125 kVp and 2.7-mm inherent aluminum-equivalent filtration combined with an additional 5.0-mm aluminum filter to simulate the radiation quality of the CT system. This is an appropriate approach because mass energy absorption coefficients for soft tissues differ by less than 4% from the corresponding value for water in the range of photon energies used for CT imaging.<sup>26</sup> As reference standard, a UNIDOS E with a Farmer chamber (TM30010; PTW Pychlau, Freiburg, Germany) with a calibration traceable back to a secondary standard (PTB, Braunschweig, Germany) was used. The Alderson

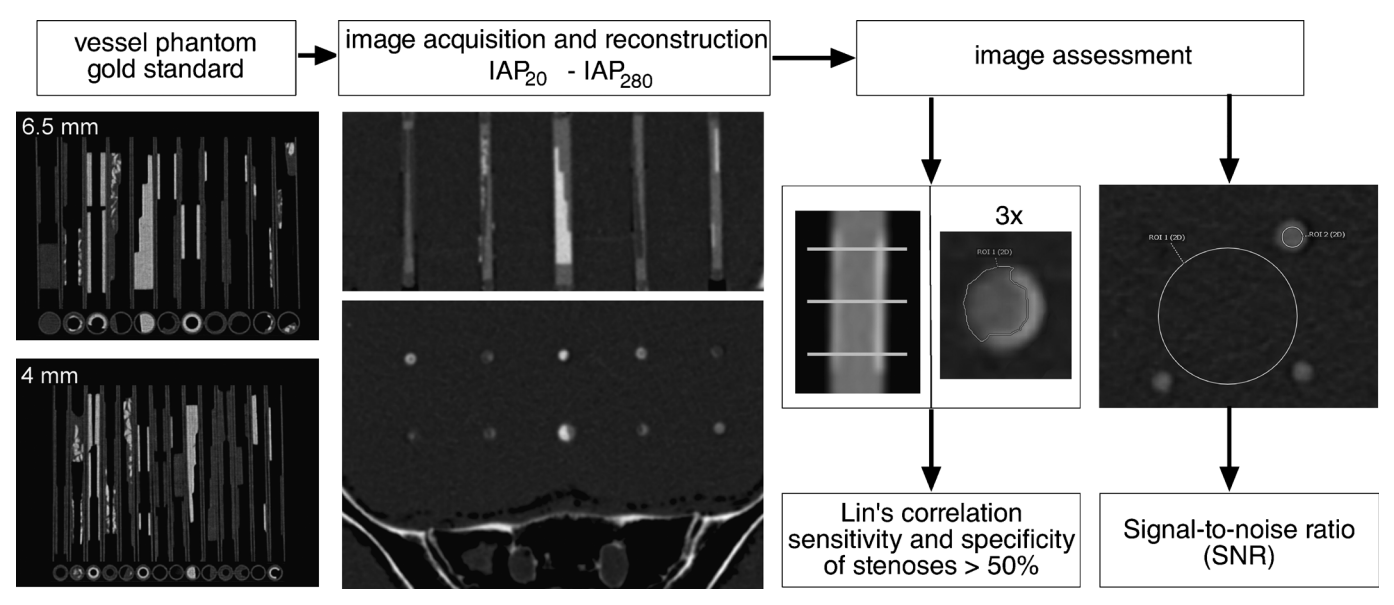


FIGURE 1. Image acquisition and assessment. Examples of the vessel phantoms measured with a high-resolution protocol (left) and placed in the Alderson phantom (middle). Mean luminal area was measured in 3 different positions for each stenosis and averaged for correlation as well as for sensitivity and specificity calculations. Luminal attenuation and standard deviation were measured in an axial plane for SNR assessment (right).

phantom was equipped with 130 TLDs distributed in all organs according to ICRP 103, excluding the salivary glands because the contribution of the head and neck to the effective dose was negligible (<1%). This whole-body TLD distribution was chosen to take internal and external scattering as well as overscanning into account. In larger organs, for example, the liver, the mean dose was calculated by averaging the values of 15 TLDs. For calibration of each measurement, 14 TLDs were exposed to a reference dose and 6 TLDs remained unexposed to estimate the background radiation for background correction. Thermoluminescence detectors were read out using an automatic Harshaw 5500 TLD-Reader within 16 hours after exposure to avoid fading. The measured electrical charge of each TLD was multiplied with a TLD-specific calibration factor obtained before to calculate the absorbed dose. To estimate the relationship between radiation dose and tube current relation of the used CT system, TLD measurements were conducted for 6 representative IAPs. The calculated mean effective dose and standard deviation was determined according to ICRP103<sup>27</sup> and compared with CTEXPO 2.0 using the average tube current.<sup>28</sup>

#### **Image Acquisition**

In this phantom study, image acquisition was conducted on a  $2\times32-\mathrm{row}$  CT (SOMATOM Definition; Siemens, Forchheim, Germany) with the following imaging parameters: tube voltage,  $120~\mathrm{kVp}$ ; collimation,  $0.6~\mathrm{mm}$ ; rotation time,  $0.3~\mathrm{seconds}$ ; pitch, 0.7; reconstructed slice thickness,  $1.0~\mathrm{mm}$ ; and reconstruction increment,  $0.7~\mathrm{mm}$ . We chose  $120~\mathrm{kVp}$  as the tube voltage because this is the current standard protocol in many institutions and is suitable for most patients.

In 8 different IAPs, the reference tube current–time product ( $I_{\rm QualRef}$ ) ranged between 20 mAs (IAP<sub>20</sub>) and 280 mAs (IAP<sub>280</sub>) to cover an exposure range between an assumed very-low-mAs and a high-dose-mAs protocol. For radiation dose estimation, 6 representative IAPs (IAP<sub>40</sub>, IAP<sub>80</sub>, IAP<sub>120</sub>, IAP<sub>160</sub>, IAP<sub>200</sub>, and IAP<sub>280</sub>) were used. For image acquisition, vessel phantoms were inserted into drilled holes of 5 and 8 mm in diameter, aligned along the z-axis at the center region of the abdominal part of the Alderson phantom (slice 29–34), and computed tomograms were acquired for IAP<sub>20</sub> to IAP<sub>280</sub> (Fig. 1). Automatic tube current modulation was applied to achieve similar noise in each xy-plane (Care Dose 4D). The image data sets were reconstructed with a standard soft kernel (B25f) as recommended by the manufacturer for vessel reconstruction and a field of view of 300 mm with a matrix size of 512  $\times$  512 pixels.

## **Image Assessment and Statistics**

The image data sets were loaded in a 3-dimensional DICOM viewer (Visage Imaging PACS 7.10, Berlin, Germany). For image quality assessment, the luminal attenuation and the image noise were measured by one author in the axial images of the vessel phantoms inserted in the Alderson phantom. Constant regions of interest (ROIs) were placed in the contrast-enhanced center of the large vessel phantoms (28 mm²) and in the center of the Alderson phantom (700 mm²) in a region with homogeneous absorption for each IAP. Mean and standard deviation CT values of the vessel lumen were recorded.

For stenosis quantification, the image data sets were assessed in random order by 2 blinded readers with 5 and 9 years of experience in

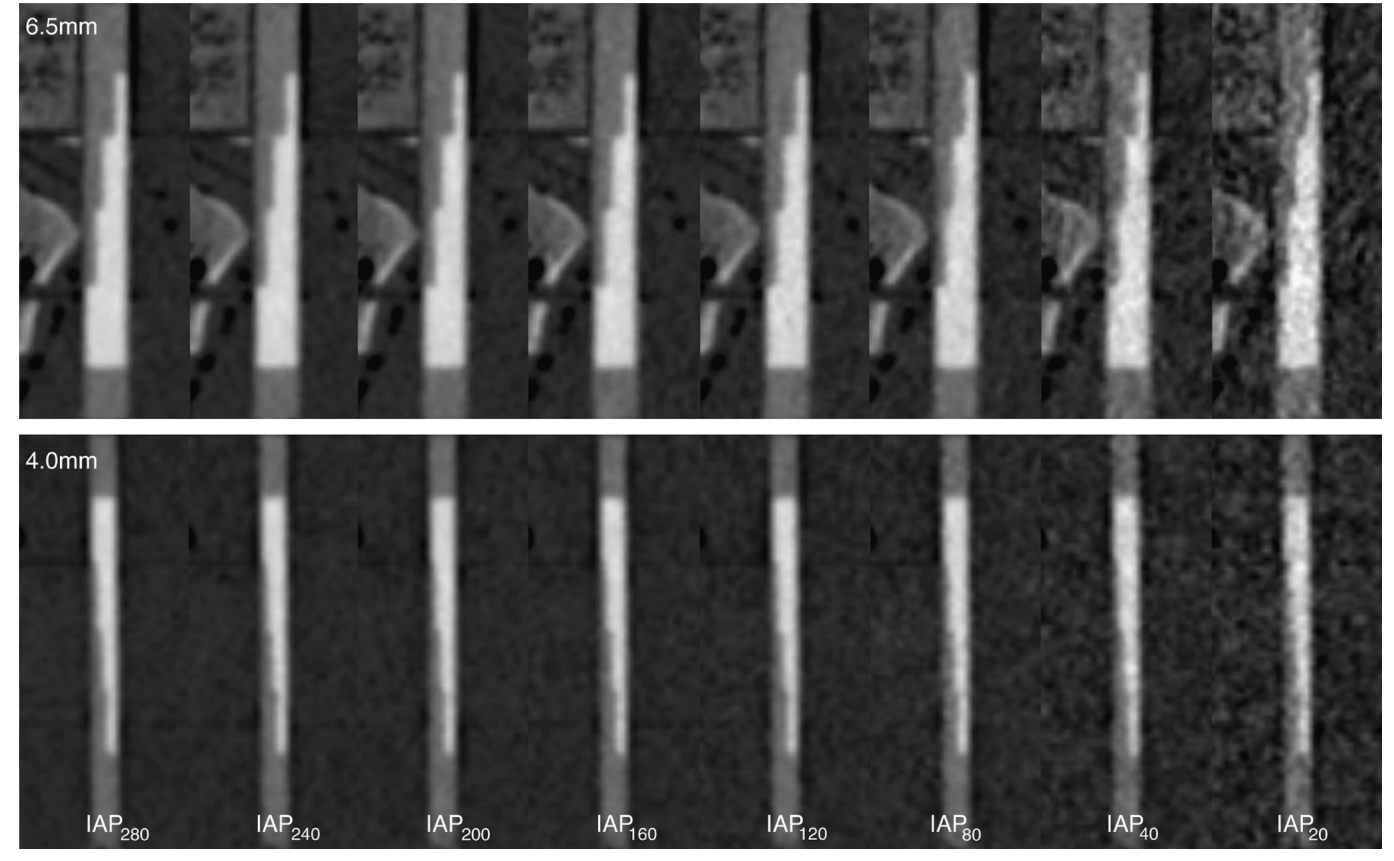


**FIGURE 2.** Large-vessel (upper half) and smalls-vessel (lower half) phantoms with a hyperdense stepwise plaque imaged with different IAPs with left highest exposition and right lowest exposition. Between IAP $_{280}$  and IAP $_{120}$ , nearly no differences in image quality are observed, whereas in IAP $_{80}$ , a slight reduction in image quality is observed. For IAP $_{40}$  and IAP $_{20}$ , a reduction in image quality is observed.

reading CTA and low-mAs CT. For image interpretation and measurement, a standard CTA window setting was provided (center/width: 400/1500 HU). Examples of stairstep-like stenoses in large and small vessel phantoms imaged with IAP20 to IAP280 are shown in Figure 2. The 2 readers measured in consensus the remaining luminal area in each stenosis by placing a freely definable ROI. If the readers did not agree, the larger ROI was chosen for further analysis. Mean luminal area measurements were recorded and repeated 3 times at different, equally spaced positions for each stenosis for averaging. In Figure 1, the image acquisition and assessment are summarized.

## **Statistics**

The statistical analysis was performed using PASW 18.0 (SPSS Inc, Chicago, IL). To assess the effect of varying tube currents, SNR was determined for each IAP to find the minimum tolerable SNR. Signal-to-noise ratio was defined as the ratio of attenuation in vessel phantom and the standard deviation of the ROI density value in the Alderson phantom. Accuracy of stenosis quantification was determined by correlation between known and measured luminal stenosis area using Lin's concordance correlation coefficient ( $\kappa_{Lin}$ ) and 95% confidence intervals dependent on vessel diameter, plaque composition, and IAPs.

In contrast to Pearson's correlation, Lin's correlation assumes a slope of 1 and zero-crossing of the line of best fit. As described previously, agreement was classified as "almost perfect" ( $\kappa_{Lin}$  values > 0.9), "substantial" ( $\kappa_{\text{Lin}}$  values of 0.8–0.9), "moderate" ( $\kappa_{\text{Lin}}$  values of 0.65–0.8), and "poor" ( $\kappa_{\text{Lin}}$  values < 0.65). <sup>29</sup> The slope of  $\kappa$  values was approximated with an exponential function. To find a reasonable tradeoff between radiation exposure and accuracy of stenosis quantification, a decrease of more than 10% below the maximum achievable correlation value was arbitrarily defined as substantial decrease in

Sensitivity, specificity, and 95% confidence intervals were calculated based on the area measurements for the detection of hemodynamically relevant stenoses (>50% luminal stenosis). For this evaluation, all plaque compositions were merged to reflect the broad spectrum of calcified and noncalcified steno-occlusive lesions in a patient population. Equivalent to Lin's correlation, a decrease of more than 10% compared with the maximum achievable sensitivity and specificity was defined as a substantial decrease in accuracy.

#### **RESULTS**

## **Radiation Dose and Overall Image Quality Assessment**

The measured effective dose ranged between  $0.8 \pm 0.2$  and 10.7± 1.1 mSv (*I*<sub>OualRef</sub>, 20–280 mAs; CTDI<sub>Vol</sub>, 1.1–12.5 mGy; Table 1)

**TABLE 1.** Image Acquisition Protocols

IAP	I <sub>QualRef,</sub> mAs	I <sub>effective</sub> , mAs	CTDI <sub>Vol,</sub> mGy	D <sub>m</sub> , mSv	D <sub>CTEXPO</sub> , mSv	SNR
IAP <sub>20</sub>	20	14	1.1	$0.8\pm0.1*$	0.7	3.4
$IAP_{40}$	40	28	1.7	$1.3\pm0.2$	1.2	5.9
$IAP_{80}$	80	55	3.6	$3.0\pm0.3$	2.8	9.1
$IAP_{120}$	120	78	5.3	$4.6\pm0.5$	4.2	11.4
$IAP_{160}$	160	104	7.1	$6.5\pm0.6$	5.5	13.4
$IAP_{200}$	200	121	8.9	$7.7 \pm 0.8$	6.9	15.2
$IAP_{240}$	240	148	10.7	$9.2 \pm 0.9*$	8.4	16.9
$IAP_{280}$	280	172	12.5	$10.7 \pm 1.1$	9.8	18.3

D<sub>m</sub> indicates measured effective radiation dose with 95% confidence intervals;  $D_{\text{CTEXPO}}$ , with CTEXPO 2.0 calculated effective dose.

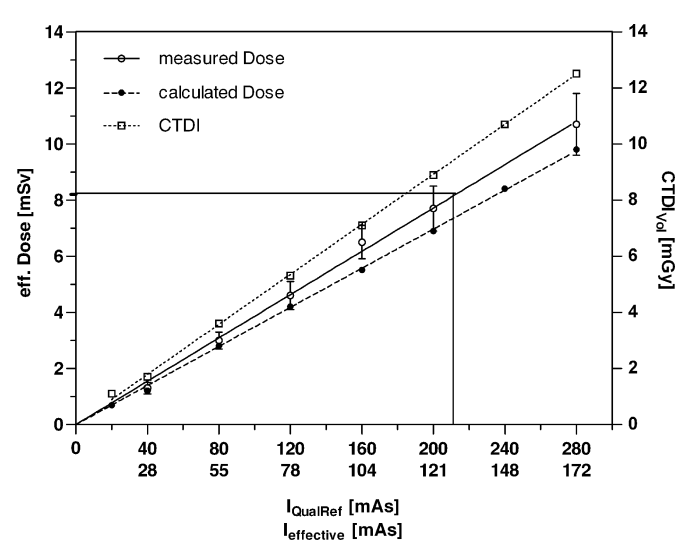


FIGURE 3. Measured effective radiation dose with 95% confidence intervals compared with CTEXPO 2.0 theoretically calculated values and  $\overrightarrow{CTDI}_{vol}$  dependent on the IAP. Measured radiation dose is approximately 10% above the theoretical values. The standard abdomen protocol (I<sub>QualRef</sub>, 210 mAs) is equivalent to  $8.2 \pm 1.0$  mSv in the used Alderson phantom.

for the chosen reference tube current-time products. The mean applied tube current ( $I_{\text{effective}}$ ) ranged between 14 and 172 mAs and was  $35\% \pm 4\%$  lower than the chosen reference tube current–time product. The corresponding estimated radiation dose in CTEXPO was approximately 10% lower (0.7-9.7 mSv). The effective dose of the clinically used standard abdomen protocol (I<sub>QualRef</sub>, 210 mAs; CTDI<sub>Vol</sub>, 9.4 mGy) was 8.2 mSv (Fig. 3).

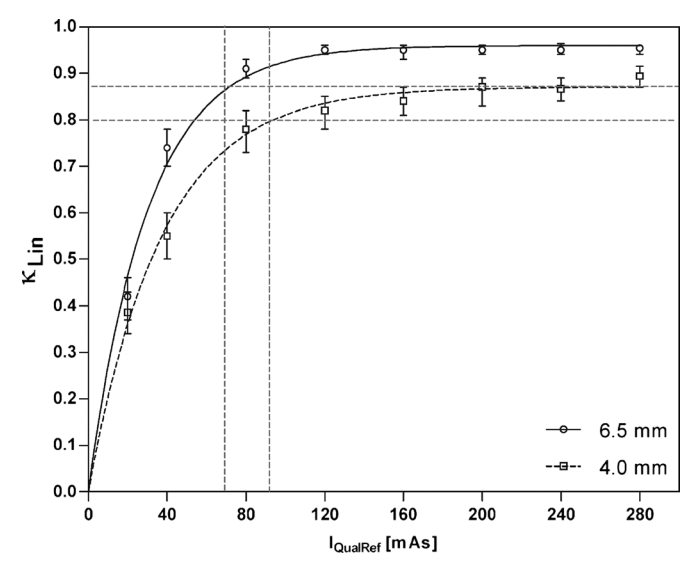


FIGURE 4. Lin's correlation of stenosis quantification was averaged over all plague compositions for each IAP dependent on the IAP and vessel phantom size. For each IAP, correlation was superior for the 6.5-mm vessel phantoms compared with the 4.0-mm vessel phantoms. A substantial decrease in correlation was observed for an  $I_{QualRef}$  of 90 mAs for the larger vessel phantoms and for an  $I_{QualRef}$  of 70 mAs for the smaller vessel phantoms (dotted line).

<sup>\*</sup>Estimated dose.

IAP	Plaque Composition						
	Average	Soft Plaque	Calcified Plaque	Inhomogeneous Plaque			
IAP <sub>20</sub>	0.42 (0.37-0.46)	0.41 (0.32-0.49)	0.58 (0.51-0.65)	0.35 (0.26-0.42)			
IAP <sub>40</sub>	0.74 (0.70-0.78)	0.79 (0.71–0.84)	0.79 (0.71-0.84)	0.62 (0.54-0.69)			
IAP <sub>80</sub>	0.91 (0.89-0.93)	0.91 (0.86-0.94)	0.92 (0.89-0.95)	0.87 (0.81-0.91)			
IAP <sub>120</sub>	0.95 (0.94-0.96)	0.96 (0.94-0.98)	0.91 (0.87-0.94)	0.93 (0.90-0.95)			
IAP <sub>160</sub>	0.95 (0.93-0.96)	0.95 (0.92-0.97)	0.93 (0.90-0.95)	0.93 (0.90-0.95)			
$IAP_{200}$	0.95 (0.94-0.96)	0.95 (0.93-0.97)	0.93 (0.89-0.95)	0.93 (0.91-0.95)			
IAP <sub>240</sub>	0.95 (0.94-0.96)	0.95 (0.92-0.96)	0.94 (0.91-0.96)	0.94 (0.91-0.96)			
IAP <sub>280</sub>	0.95 (0.94-0.96)	0.95 (0.92-0.97)	0.94 (0.91-0.96)	0.94 (0.91-0.96)			

TABLE 2. Lin's Correlation Coefficient of Stenosis Quantification for 6.5-mm Vessels

Data are presented as  $\kappa_{Lin}$  (95% CI).

95% CI indicates 95% confidence interval.

The highest SNR was observed for the highest effective dose. The SNR decreased nearly linearly to 80 mAs and deteriorated rapidly at settings below 80 mAs (Table 1).

#### **Stenoses Quantification**

The quality of stenosis quantification was assessed in a total of 2592 stenosis measurements (108 stenoses were measured 3 times for each of the 8 IAPs).

The correlation averaged over all plaque compositions was, for each IAP, superior for 6.5-mm vessel phantom stenoses as compared with 4.0-mm vessel phantoms, as shown in Figure 4. The best correlation for both vessel phantom diameters was noted for the IAP with highest reference tube current–time product (6.5 mm, 0.95  $\pm$  0.01; 4.0 mm, 0.89  $\pm$  0.02). In large vessel phantoms (6.5 mm), the correlation decreased slightly with reduced tube current but was still noted to be almost perfect for IAP<sub>80</sub> to IAP<sub>280</sub> ( $\kappa_{\rm Lin}=0.91$ –0.95). For IAP<sub>40</sub>, the correlation decreased to moderate values ( $\kappa_{\rm Lin}=0.74$ ) and poor values for IAP<sub>20</sub> ( $\kappa_{\rm Lin}=0.42$ ). In 4-mm vessel phantoms, the best correlation was also observed for the highest exposition level

(IAP<sub>280</sub>,  $\kappa_{Lin}=0.89$ , substantial correlation). For the tube current–reduced acquisition protocols IAP<sub>240</sub> to IAP<sub>120</sub>, the correlation values remained substantial (IAP<sub>120</sub>,  $\kappa_{Lin}=0.82$ ). The correlation decreased to moderate values for IAP<sub>80</sub> ( $\kappa_{Lin}=0.78$ ) and to poor values for the low-mAs protocols IAP<sub>40</sub> ( $\kappa_{Lin}=0.55$ ) and IAP<sub>20</sub> ( $\kappa_{Lin}=0.39$ ).

In the subgroup analysis for the 3 different plaque types, differences were low in large vessels between IAP<sub>280</sub> and IAP<sub>120</sub> ( $\kappa_{\rm Lin}=0.91$ –0.96). For IAP<sub>80</sub> and IAP<sub>40</sub>, luminal delineation was superior for homogeneous hypodense and hyperdense plaques stenoses (IAP<sub>40</sub>,  $\kappa_{\rm Lin}=0.79$ ; IAP<sub>80</sub>,  $\kappa_{\rm Lin}=0.91$ –0.92) compared with inhomogeneous plaque stenoses (IAP<sub>40</sub>,  $\kappa_{\rm Lin}=0.62$ ; IAP<sub>80</sub>,  $\kappa_{\rm Lin}=0.87$ ) (Table 2, Fig. 5A). In 4-mm vessel phantoms, the correlation for hyperdense plaque stenoses was superior for each IAP compared with inhomogeneous and hypodense plaque compositions, which showed very similar correlation as shown in Figure 5B and Table 3. According to the defined threshold, a substantial deterioration of correlation was observed below a current-time product of approximately 90 mAs (SNR, 9.1) for large vessel phantoms and 120 mAs (SNR, 10.8) for small vessel phantoms.

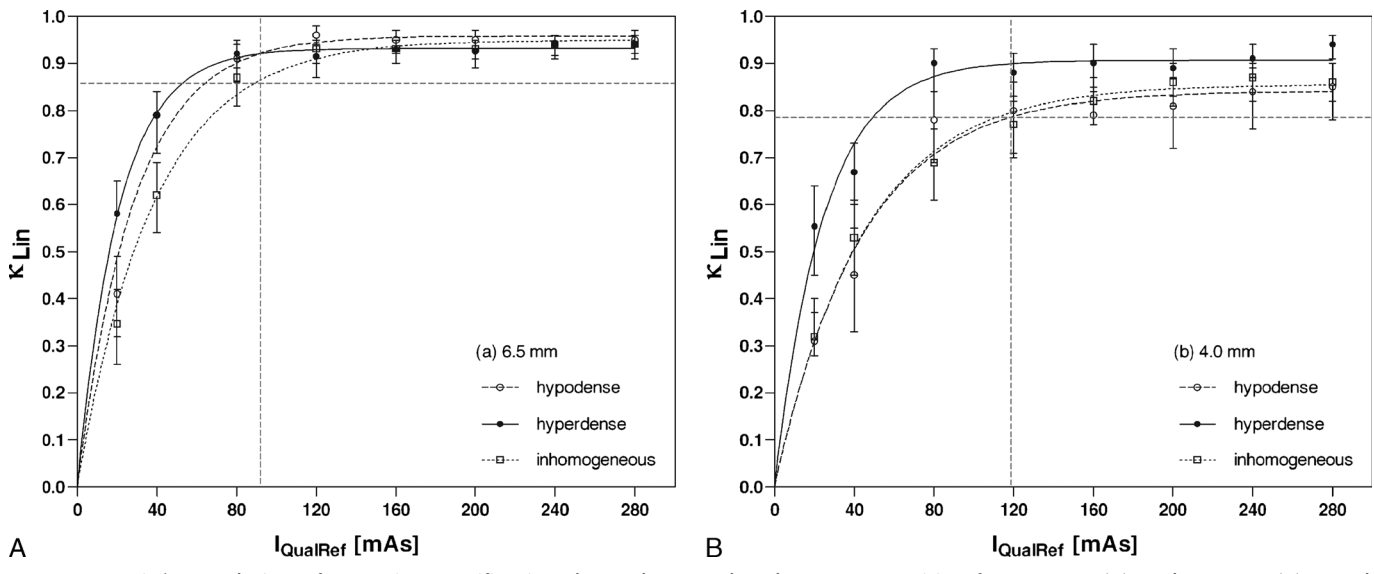


**FIGURE 5.** Lin's correlation of stenosis quantification dependent on the plaque composition for 6.5-mm (A) and 4.0-mm (B) vessel phantoms. The lowest correlation for both vessel diameters is observed for the inhomogeneous plaques stenoses, which therefore limit the dose reduction possibilities to an  $I_{QualRef}$  of 90 mAs for the large and  $I_{QualRef}$  of 120 mAs for the small vessel phantoms (dashed line).

TABLE 3. Lin's Correlation Coefficient of Stenosis Quantification for 4.0-mm Vessels

IAP	Plaque Composition					
	Average	Soft Plaque	Calcified Plaque	Inhomogeneous Plaque		
IAP <sub>20</sub>	0.39 (0.34-0.43)	0.31 (0.21-0.40)	0.55 (0.45-0.64)	0.32 (0.28–0.37)		
IAP <sub>40</sub>	0.55 (0.50-0.60)	0.45 (0.33–0.55)	0.67 (0.60-0.73)	0.53 (0.45-0.61)		
IAP <sub>80</sub>	0.78 (0.73-0.82)	0.78 (0.69-0.84)	0.90 (0.84-0.93)	0.69 (0.61-0.76)		
IAP <sub>120</sub>	0.82 (0.78-0.85)	0.80 (0.71-0.86)	0.88 (0.82-0.92)	0.77 (0.70-0.83)		
$IAP_{160}$	0.84 (0.81-0.87)	0.79 (0.79–0.85)	0.90 (0.84-0.94)	0.82 (0.77–0.87)		
$IAP_{200}$	0.87 (0.83-0.89)	0.81 (0.72-0.87)	0.89 (0.83-0.93)	0.86 (0.81-0.90)		
$IAP_{240}$	0.87 (0.84–0.89)	0.84 (0.76-0.89)	0.91 (0.87-0.94)	0.87 (0.82-0.90)		
IAP <sub>280</sub>	0.89 (0.87–0.91)	0.85 (0.78–0.90)	0.94 (0.91–0.96)	0.86 (0.82–0.90)		

Data are presented as  $\kappa_{Lin}$  (95% CI).

95% CI indicates 95% confidence interval.

Sensitivity and specificity values for the detection of stenoses of greater than 50% are shown in Figure 6. The sensitivity for the detection of hemodynamically relevant stenoses remained high in large and small vessels for all IAPs (IAP<sub>20</sub>-IAP<sub>280</sub>, 90%-99%). The overestimation of nonhemodynamic relevant stenoses as expressed by the specificity showed a considerable dose dependency as shown in Figure 6. In 4-mm vessel phantoms, an overestimation of the stenoses was more often observed as compared with large phantoms for each IAP, resulting in a lower specificity for each IAP in the smaller phantoms. The highest specificity values were observed for the IAP with the highest exposition (4 mm, 0.81; 6.5 mm, 0.96) and decreased remarkably with tube current reduction. A substantial loss of specificity was achieved at an I<sub>QualRef</sub> of 100 mAs (SNR, 9.7) and lower for large vessel phantoms and at an  $I_{\text{OualRef}}$  of 130 mAs (SNR, 11.3) for the small vessel phantoms.

## **DISCUSSION**

The results of our phantom study suggest that if arterial vessel depiction is the main imaging task of an abdominal CT examination, a substantial tube current reduction as compared with the standard abdominal CT protocol is feasible. The possible tube current reduction in CTA as compared with the standard protocol depends on the arterial vessel size and the image noise that is accepted by the reader. These findings underline the importance of optimizing scan protocols with respect to the specific imaging task to follow the ALARA principle as close as possible.

For this study, we used a phantom-based study approach because it has 2 major advantages when compared with a patient study. First, the results can be compared with a true gold standard because the geometrical properties of the vessel phantoms are known in detail. In contrast, patient studies of CTA in steno-occlusive disease are usually limited by the lack of a true gold standard. Even in cases where digital substraction angiography is available, the comparison between cross-sectional and projection imaging is challenging and prone to errors. Second, a phantom study allows for a systematic analysis of a broad variety of scan parameters that would not be possible in a patient study. Another advantage of this phantom-based approach is that it represents the qualitative and clinically relevant aspects of stenosis depiction by the radiologist as compared with the SNR and modulation transfer function measurements with technical phantoms, which allow to characterize only the physical characteristics of the imaging system.30

In our experimental setting, 2 vessel diameters with stenoses ranging from 10% to occlusion with 3 plaque compositions (soft, calcified, and inhomogeneous plaques) were simulated. The absorp-

tion of the plaques was in good agreement with values obtained from a previous patient study.<sup>31</sup> Because of technical limitations, the density of calcified plaques was limited to 1000 HU compared with in vivo values ranging up to 1900 HU.<sup>31</sup> Compared with Perisinakis et al,<sup>22</sup> not only circular in-stent stenosis but also more complex stenoses with inhomogeneous plaques were simulated.

The luminal enhancement of 350 HU was chosen according to values known from clinical studies.<sup>25</sup> This phantom design allowed for a precise correlation of measured stenosis area with the known geometric properties of the phantom. The clinically used diameter measurements were omitted, because stenosis area measurements represents the complex stenosis configuration more realistically compared with diameter measurements.

In this study, the optimal correlation of stenosis quantification was, as expected, observed for the highest radiation dose. A substantial reduction of 10% in the correlation as compared with the maximal achievable correlation was observed for large vessel phantoms, with all plaque compositions merging at an  $I_{\rm QualRef}$  of 70 mAs, and for the smaller vessels, at an  $I_{\rm QualRef}$  of 100 mAs. This reflects the lower effect of SNR on the stenosis quantification for larger vessels (Fig. 4).

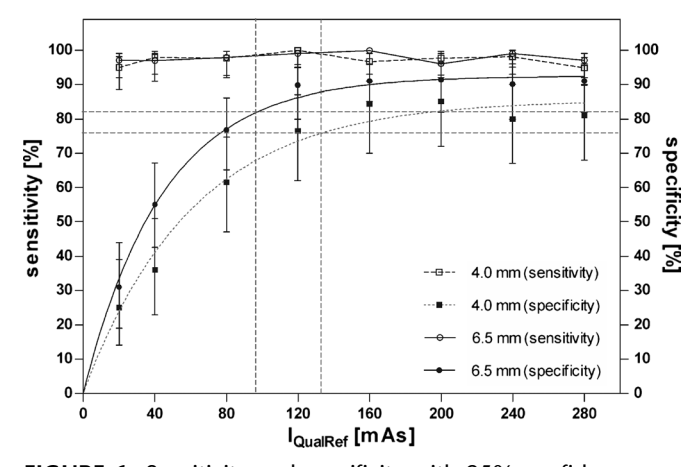


FIGURE 6. Sensitivity and specificity with 95% confidence intervals for the detection of hemodynamically relevant stenoses. All plaque compositions were merged to reflect the broad spectrum of steno-occlusive lesions in a patient population. The substantial loss of specificity is observed for the large vessel phantoms at an  $I_{QualRef}$  of 80 mAs and for the small vessel phantoms at an  $I_{OualRef}$  of 130 mAs (dashed line).

Considering the plaque composition, the lowest correlation was observed for inhomogeneous plaque stenoses (Figs. 5A, B) because a visual separation of the inhomogeneous plaque material and the contrast-enhanced lumen is difficult. In the clinical setting, a reliable stenosis quantification is essential. Because the composition of plaques is unpredictable in most cases, especially the results obtained for the inhomogeneous plaques have to be taken into account when dose reduction is applied.

The results for sensitivity and specificity are in good agreement with the results for dose reduction obtained with Lin's correlation. A substantial decrease in specificity compared with maximum specificity was observed for large vessel phantoms at an  $I_{\text{OualRef}}$  of 90 mAs and for small vessel phantoms at an  $I_{\text{QualRef}}$  of 130 mAs. If tube current is further reduced, the noise increases and the luminal delineation is reduced, as demonstrated by the correlation results. The increase in image noise at lower exposition leads to an overestimation of stenoses grading caused by the inhomogeneous appearance of the vessel lumen and thus results in lower specificity while the sensitivity remains high for all IAP.

All phantom measurements were conducted in an anthropomorphic Alderson phantom with TLD dosimetry to simulate the radiation quality in human beings and to measure the radiation exposure to estimate the effective dose. The measured effective dose in this study for a standard abdominal study was in the lower range compared with literature values, 32,33 mainly because of the slim habitus of the Alderson phantom and the automatic tube current modulation. As compared with the theoretical approximation with CTEXPO, the measured exposition was 10% higher, which is in good agreement with published values.<sup>26</sup> Reasons for this difference can be addressed by the use of a mean tube current for calculation of the radiation exposure and differences between the mathematical phantom ADAM used in CTEXPO compared with the Alderson phantom.<sup>26</sup>

Our results show that a tube current reduction of approximately 43% to 4.6 mSv with IAP<sub>120</sub> as compared with the standard abdominal protocol with the standard tube voltage is possible. This is in good accordance with the results of Fraioli et al, 19 who showed with a 4-row CT and a 2.5-mm collimation without tube current modulation that low-mAs CTA is possible in a rtic and lower extremity arteries with 3.7 mSv as compared with standard abdominal CT with 13.7 mSv. Our results also confirm the results from Perisinakis et al<sup>22</sup> that in vessels with a circular shape, low-mAs protocol is feasible, which is, however, limited, as demonstrated in this study if an inhomogeneous unknown plaque structure is present.

Several potential limitations of our study merit consideration. First, all phantoms were rigid, not simulating any cardiac-induced vessel motion, and all phantoms were measured in the best orientation, possibly overestimating the results. Second, the Alderson phantom simulates only 1 patient habitus. However, because of the use of the automatic exposure control, the image noise index should be comparable in other patient sizes. Third, the tube voltage was set to 120 kVp because this tube voltage is the standard setting in many institutions, as it is principally suitable for patients of different body habitus. A further dose reduction may be possible with low-kVp protocols, which results in higher iodine absorption and higher image noise but together may provide diagnostically acceptable images. However, it would not have changed the relative dependency of the tube current product on the image quality in CTA. In addition, the use of lower tube voltages is applicable only in slim patients because of tube current limitations. Therefore, the study was limited to the standard tube voltage, but the results obtained for 120 kVp may suggest the imaging parameters for lower tube voltages to optimize the application of radiation dose. Furthermore, only 1 reconstruction algorithm with 1 reconstruction matrix size was investigated. A harder reconstruction kernel may, on the one hand, increase the luminal delineation for the high-contrast phantoms, but on the other hand, it

increases the image noise. Therefore, a harder kernel may lead to higher needed radiation exposure to preserve the SNR.<sup>23</sup> This effect may be reduced by adding new iterative reconstruction algorithms in the future.20

Finally, we arbitrarily defined a 10% loss in correlation, specificity, and sensitivity as acceptable for our tube current-reduced

In conclusion, CTA represents a high-object-contrast scenario comparable with virtual colonoscopy and lung CT-with a high potential for dose reduction while maintaining a high diagnostic accuracy. To ensure a reliable diagnostic quality in CTA, the most challenging small vessels with heterogeneous plaque composition have to be assessable. Our study suggests that the SNR should not fall below 10.8 for the used standard soft reconstruction kernel, which allows a considerably tube current reduction compared with a standard abdominal study protocol.

## **Clinical Impact**

In abdominal CTA, a considerable reduction in radiation exposure as compared with an abdominal standard protocol is feasible. The extent of the dose reduction is dependent on the size of the vessel to be depicted.

#### REFERENCES

- 1. Albrecht T, Foert E, Holtkamp R, et al. 16-MDCT angiography of aortoiliac and lower extremity arteries: comparison with digital subtraction angiography. AJR Am J Roentgenol. 2007;189:702-711.
- 2. Met R, Bipat S, Legemate DA, et al. Diagnostic performance of computed tomography angiography in peripheral arterial disease: a systematic review and meta-analysis. JAMA. 2009;301:415-424.
- 3. Rountas C, Vlychou M, Vassiou K, et al. Imaging modalities for renal artery stenosis in suspected renovascular hypertension: prospective intraindividual comparison of color Doppler US, CT angiography, GD-enhanced MR angiography, and digital substraction angiography. Ren Fail. 2007;29:295-302.
- Wittenberg G, Kenn W, Tschammler A, et al. Spiral CT angiography of renal arteries: comparison with angiography. Eur Radiol. 1999;9:546-551
- 5. Levin DC, Rao VM, Parker L, et al. The effect of the introduction of MR and CT angiography on the utilization of catheter angiography for peripheral arterial disease. J Am Coll Radiol. 2007;4:457-460.
- 6. Leiner T, Kessels AGH, Nelemans PJ, et al. Peripheral arterial disease: comparison of color duplex US and contrast-enhanced MR angiography for diagnosis. Radiology. 2005;235:699-708.
- 7. Ouwendijk R, de Vries M, Pattynama PM, et al. Imaging peripheral arterial disease: a randomized controlled trial comparing contrast-enhanced MR angiography and multi-detector row CT angiography. Radiology. 2005;236:1094-1103.
- 8. Lee CH, Goo JM, Ye HJ, et al. Radiation dose modulation techniques in the multidetector CT era: from basics to practice. Radiographics. 2008;28: 1451-1459.
- 9. Prakash P, Kalra MK, Kambadakone AK, et al. Reducing abdominal CT radiation dose with adaptive statistical iterative reconstruction technique. Invest Radiol. 2010;45:202-210.
- 10. Deak PD, Langner O, Lell M, et al. Effects of Adaptive Section Collimation on Patient Radiation Dose in Multisection Spiral CT1. Radiology. 2009;252: 140-147
- 11. May MS, Wust W, Brand M, et al. Dose reduction in abdominal computed tomography: intraindividual comparison of image quality of full-dose standard and half-dose iterative reconstructions with dual-source computed tomography. Invest Radiol 2011:46:465-470
- 12. Winklehner A, Goetti R, Baumueller S, et al. Automated attenuation-based tube potential selection for thoracoabdominal computed tomography angiography: improved dose effectiveness. Invest Radiol. 2011;46:767–773.
- 13. Papadakis AE, Perisinakis K, Oikonomou I, et al. Automatic exposure control in pediatric and adult computed tomography examinations: can we estimate organ and effective dose from mean MAS reduction? Invest Radiol. 2011;46: 654-662
- 14. McCollough CH, Primak AN, Braun N, et al. Strategies for reducing radiation dose in CT. Radiol Clin North Am. 2009;47:27-40.
- 15. Kubo T, Lin PJ, Stiller W, et al. Radiation dose reduction in chest CT: a review. AJR Am J Roentgenol. 2008;190:335-343.
- 16. Iannaccone R, Laghi A, Catalano C, et al. Detection of colorectal lesions: lowerdose multi-detector row helical CT colonography compared with conventional colonoscopy. Radiology. 2003;229:775-781.
- 17. Kim SH, Lee JM, Shin C-I, et al. Effects of spatial resolution and tube current on computer-aided detection of polyps on CT colonographic images: phantom study. Radiology. 2008;248:492-503

- 18. Watanabe H, Kanematsu M, Miyoshi T, et al. Improvement of image quality of low radiation dose abdominal CT by increasing contrast enhancement. AJR Am J Roentgenol. 2010;195:986–992.
- 19. Fraioli F, Catalano C, Bertoletti L, et al. Multidetector-row CT angiography of renal artery stenosis in 50 consecutive patients: prospective interobserver comparison with DSA. Radiol Med. 2006;111:459-468.
- 20. Sahani DV, Kalva SP, Hahn PF, et al. 16-MDCT angiography in living kidney donors at various tube potentials: impact on image quality and radiation dose. AJR Am J Roentgenol. 2007;188:115–120.
- 21. Fraioli F, Catalano C, Napoli A, et al. Low-dose multidetector-row CT angiography of the infra-renal agrta and lower extremity vessels; image quality and diagnostic accuracy in comparison with standard DSA. Eur Radiol. 2006;16: 137-146.
- 22. Perisinakis K, Manousaki E, Zourari K, et al. Accuracy of multislice CT angiography for the assessment of in-stent restenoses in the iliac arteries at reduced dose: a phantom study. Br J Radiol. 2011;84:244–250.
- Kaempf M, Ketelsen D, Syha R, et al. CT angiography of various superficial femoral artery stents: an in vitro phantom study. Eur J Radiol. 2012;81: 1584-1588.
- 24. Werncke T, Albrecht T, Wolf KJ, et al. Dual energy CT of the peripheral arteries: a phantom study to assess the effect of automatic plaque removal on stenosis grading. Rofo. 2010;182:682-689.
- 25. Meyer BC, Oldenburg A, Frericks BB, et al. Quantitative and qualitative evaluation of the influence of different table feeds on visualization of peripheral arteries in CT angiography of aortoiliac and lower extremity arteries. Eur Radiol. 2008;18:1546-1555.

- 26. Lechel U, Becker C, Langenfeld-Jager G, et al. Dose reduction by automatic exposure control in multidetector computed tomography: comparison between measurement and calculation. *Eur Radiol*. 2009;19:1027–1034.
- 27. ICRP. The 2007 recommendations of the International Commission on Radiological Protection. ICRP publication 103. Ann ICRP. 2007;37:1-332.
- 28. Stamm G, Nagel HD. CT-Expo-ein neuartiges Programm zur Dosisevaluierung in der CT. Rofo. 2002;174:1570-1576.
- 29. Lin L, Torbeck LD. Coefficient of accuracy and concordance correlation coefficient: new statistics for methods comparison. PDA J Pharm Sci Technol. 1998;52:55-59
- 30. Schindera ST, Nelson RC, Yoshizumi T, et al. Effect of automatic tube current modulation on radiation dose and image quality for low tube voltage multidetector row CT angiography: phantom study. Acad Radiol. 2009;16:997-1002.
- 31. Toussaint ND, Lau KK, Strauss BJ, et al. Determination and validation of aortic calcification measurement from lateral bone densitometry in dialysis patients. Clin J Am Soc Nephrol. 2009;4:119-127.
- 32. Fujii K, Aoyama T, Yamauchi-Kawaura C, et al. Radiation dose evaluation in 64-slice CT examinations with adult and paediatric anthropomorphic phantoms. Br J Radiol. 2009;82:1010-1018
- 33. Van der Molen AJ, Veldkamp WJ, Geleijns J. 16-slice CT: achievable effective doses of common protocols in comparison with recent CT dose surveys. Br J Radiol. 2007;80:248-255.
- 34. Cho ES, Chung TS, Oh DK, et al. Cerebral computed tomography angiography using a low tube voltage (80 kVp) and a moderate concentration of iodine contrast material: a quantitative and qualitative comparison with conventional computed tomography angiography. Invest Radiol. 2012;47:142-147.